Research Square

Preprints are preliminary reports that have not undergone peer review.
They should not be considered conclusive, used to inform clinical practice,
or referenced by the media as validated information.

Spatial Transcriptomic Prioritization of Anesthesia-Associated Candidate Genes in Triple-Negative Breast Cancer: An Exploratory Multi-Omics Reappraisal

Weixian Xie

2026691021@gzhmu.edu.cn

Affiliated Qingyuan Hospital,Guangzhou Medical University,Qingyuan People's Hospital

Wenyue Xiang

Affiliated Qingyuan Hospital,Guangzhou Medical University,Qingyuan People's Hospital

Zhiming Huang

Affiliated Qingyuan Hospital,Guangzhou Medical University,Qingyuan People's Hospital

Research Article

Keywords: triple-negative breast cancer, anesthesia-associated genes, spatial transcriptomics, Mendelian randomization resources, tumor immune microenvironment, SDC1, CD44

Posted Date: September 9th, 2026

DOI: https://doi.org/10.21203/rs.3.rs-10830074/v1

License: This work is licensed under a Creative Commons Attribution 4.0 International License.
Read Full License

Additional Declarations: No competing interests reported.

Version of Record: A version of this preprint was published at BMC Cancer on November 3rd, 2026. See the published version at https://doi.org/10.1186/s12885-026-17307-1.

Abstract

Background

Perioperative anesthetic exposure has been linked to tumor biology in experimental and clinical studies, but public-data analyses can overstate causal and clinical implications when genetic instruments, disease endpoints and validation datasets are incomplete. Triple-negative breast cancer (TNBC) remains an aggressive breast cancer subtype with substantial immune and stromal heterogeneity. We performed a conservative multi-omics reappraisal of anesthesia-associated candidate genes in TNBC, emphasizing evidence that could be supported by the available public datasets.

Methods

Thirty-nine anesthesia-associated genes were curated from public gene-disease and toxicogenomic resources. Genetic evidence was audited using available breast cancer GWAS and eQTL resources, with Mendelian randomization (MR), SMR and colocalization outputs classified by data completeness and interpretability. TNBC spatial transcriptomics from GSE210616 was analyzed at the patient level across three Visium samples and 5,103 spots. Moran's I was summarized per patient and combined using meta-analytic evidence. TLS-associated transcriptional hotspots, spatial niches and ligand-receptor co-expression were evaluated with explicit recognition that spots are technical observations nested within patients.

Results

The genetic evidence did not support a definitive causal claim for the main TNBC candidates. In the analyzed MR resources, a complete pipeline-level result was available for SCN9A, whereas corresponding complete eQTL-supported MR results were not available for SDC1, ZNF521, LPO, TRPA1 and GSDME. Spatial transcriptomics provided the strongest directly usable evidence. SDC1 showed consistent positive spatial autocorrelation in all three TNBC patients, with a mean Moran's I of 0.3042 and a patient-level Stouffer meta-analysis P value of 7.92e-06. TLS-associated transcriptional hotspots comprised 192 of 5,103 spots (3.8%) and were patient-dependent, with 125, 67 and 0 hotspot spots in the three samples. SDC1 expression was higher in TLS-associated hotspots (P = 5.75e-11), and SDC1-CD44 spatial co-expression was positive (Spearman r = 0.3307, P = 1.69e-130). In contrast, SDC1 showed weak negative correlation with the M2 macrophage score (Spearman r=-0.0336, P = 0.0165), indicating that this axis is not supported as a strong positive macrophage mechanism.

Conclusions

The available evidence supports an exploratory spatial and genetic-prioritization study rather than a definitive causal study of anesthesia-driven TNBC metastasis. SDC1 is the most supportable candidate because it shows consistent patient-level spatial clustering and TLS-associated spatial enrichment in TNBC tissue. Further TNBC-specific genetic outcomes, independent external cohorts and experimental validation are needed before clinical or mechanistic claims can be made.

1. Introduction

Triple-negative breast cancer is defined by the lack of estrogen receptor, progesterone receptor and HER2 expression [3, 8]. It is clinically aggressive, molecularly heterogeneous and associated with high recurrence risk, particularly during the first several years after diagnosis [7]. The immune and stromal composition of TNBC tissue has also become increasingly important because tumor-infiltrating lymphocytes, tertiary lymphoid structures and macrophage states can influence prognosis and response to therapy [6, 10].

Perioperative anesthetic exposure has been proposed to influence tumor biology through effects on inflammation, immune surveillance, hypoxia, ion channels and cellular stress responses. Experimental data have suggested plausible links between anesthetic agents and proliferation, migration or immune modulation. However, clinical outcome studies and genetic epidemiology require careful interpretation because breast cancer subtype, endpoint definition, treatment context and tumor microenvironment can strongly modify observed associations [12].

Mendelian randomization can help prioritize potential causal genes when valid genetic instruments and appropriate outcomes are available [4, 5]. Colocalization and SMR can further assess whether expression quantitative trait loci and disease associations are likely to share a causal signal [15, 17]. These approaches become less secure when the available outcome is overall breast cancer rather than TNBC-specific metastasis or recurrence, when gene-level eQTL instruments are incomplete, or when drug-target labels are treated as causal drug exposure without appropriate pQTL or pharmacologic instruments.

Spatial transcriptomics provides complementary information by preserving tissue architecture [1, 13]. It can show whether candidate genes are spatially clustered, whether their expression aligns with immune or stromal niches, and whether computational TLS-associated regions contain specific candidate gene patterns. For TNBC, patient-level spatial analysis is particularly important because treating thousands of tissue spots as independent biological replicates can inflate precision.

The present study therefore reappraises anesthesia-associated candidate genes in TNBC using a conservative evidence framework. The goal is not to prove that anesthetic exposure causes TNBC metastasis, but to identify which anesthesia-associated genes remain plausible candidates after genetic evidence audit and patient-level spatial transcriptomic evaluation.

2. Materials and Methods

2.1 Candidate gene curation

Anesthesia-associated candidate genes were curated from public gene-disease and toxicogenomic resources using anesthesia-related search terms. Genes were retained when they were linked to anesthetic agents, perioperative pharmacology or anesthesia-related biologic processes. The final candidate set contained 39 genes spanning ion channels, inflammatory mediators, oxidative stress genes and immune-related markers.

2.2 Genetic evidence sources and classification

Breast cancer GWAS summary statistics included GWAS Catalog accession GCST010098, representing overall breast cancer rather than a TNBC-specific metastasis or recurrence endpoint [16]. eQTL resources included accessible eQTLGen-derived and tissue-level files [9, 14]. Genetic results were classified according to endpoint specificity, instrument availability, source-data traceability and internal consistency, and were interpreted as complete, exploratory or unsupported evidence.

Because the retained GWAS endpoint was not TNBC-specific metastasis, genetic associations were not interpreted as direct evidence for TNBC metastatic causality. Where complete real-data gene-level MR output was absent for a candidate gene, that gene was not described as genetically validated.

2.3 MR, SMR and colocalization review

MR, SMR and colocalization tables were checked for gene identity, effect estimate consistency, P values, Bonferroni or FDR interpretation, and source-data traceability. Results were retained only as exploratory candidate-prioritization evidence when the relevant exposure instruments, outcome endpoint and supporting eQTL or pQTL data were not complete. Colocalization evidence was similarly treated as supportive only when the signal source was traceable and internally consistent.

2.4 Drug-target and mediation evidence

Drug-target outputs were treated as gene-drug annotation rather than causal drug-target MR unless supported by appropriate pharmacologic or protein instruments. Mediation outputs were retained only as hypothesis-generating because some proportions were unstable, negative or greater than 100%, which can occur when assumptions are not met or when total and indirect effects are imprecise.

2.5 Spatial transcriptomics data

TNBC spatial transcriptomics data were obtained from GSE210616. The analyzed subset included three TNBC Visium samples and 5,103 tissue spots. Standard quality-control and normalization procedures were applied before candidate gene expression, immune score, spatial niche and co-expression analyses. Patient identity was treated as the biological replication unit.

2.6 Patient-level spatial autocorrelation

Spatial autocorrelation was assessed using Moran's I for candidate genes within each patient [11]. Results were summarized as patient-specific Moran's I values, directional consistency across patients, number of patients with FDR < 0.05 and Stouffer meta-analysis P values. Combined spot-level significance alone was not used as the main inferential unit.

2.7 TLS-associated transcriptional hotspot analysis

TLS-associated transcriptional hotspots were defined computationally using marker-based TLS-related expression patterns. These regions were described as TLS-associated transcriptional hotspots rather than pathology-confirmed tertiary lymphoid structures. Hotspot counts and proportions were reported overall and per patient to preserve between-patient heterogeneity.

2.8 Spatial niche and ligand-receptor co-expression analyses

Spatial niches were assigned using expression-based neighborhood and marker patterns. Candidate gene expression was compared across niches and between TLS-associated hotspot and non-hotspot spots. SDC1-CD44 spatial co-expression and selected immune-marker correlations were evaluated using Spearman correlation. Co-expression was interpreted as spatial association, not proof of ligand-receptor activation.

2.9 Statistical reporting

Continuous values are reported as effect estimates, correlation coefficients, Moran's I values or mean differences where appropriate. Multiple-testing results were interpreted using FDR or Bonferroni correction according to the relevant analysis [2]. For analyses conducted at spot level, patient-level consistency and biological replication were emphasized in interpretation.

3. Results

3.1 Genetic evidence required conservative interpretation

The evidence audit changed the strength of several original claims. A complete real-data MR pipeline-level result was available for SCN9A. However, corresponding complete eQTL-supported MR results for the main manuscript candidates SDC1, ZNF521, LPO, TRPA1 and GSDME were not available in the analyzed resources. Therefore, these genes were not interpreted as confirmed MR-supported TNBC causal genes.

Colocalization summaries were also inconsistent across output sources. Some enhanced colocalization summaries suggested high PP.H4 values, but the corresponding real-data and integrated evidence outputs did not consistently support those signals for all core genes. These results were therefore retained as exploratory prioritization evidence rather than definitive shared-causal-signal evidence.

3.2 SDC1 showed the most consistent patient-level spatial clustering

Spatial transcriptomics provided the strongest directly supportable result. SDC1 showed positive Moran's I values in all three TNBC patients, with a mean Moran's I of 0.3042 and a range of 0.2261 to 0.3948. All three patients showed FDR < 0.05, and patient-level Stouffer meta-analysis supported a consistent spatial signal (P = 7.92e-06). Among the evaluated candidate genes, this made SDC1 the most stable spatial candidate.

Other genes showed weaker or more patient-dependent signals. ZNF521 had a mean Moran's I of 0.0162 and positive direction in two of three patients. LPO, TRPA1 and GSDME showed mixed signals across patients, supporting exploratory but not definitive interpretation.

3.3 TLS-associated transcriptional hotspots were present but heterogeneous

The optimized TLS-associated hotspot analysis identified 192 hotspot spots among 5,103 total spots, corresponding to 3.8% of analyzed spots. Hotspots were unevenly distributed across patients, with 125, 67 and 0 hotspot spots in the three TNBC samples. This finding supports the presence of TLS-associated transcriptional structure in a subset of samples, but it also shows that TLS-associated regions are patient-dependent and should not be described as uniformly present across all TNBC cases.

SDC1 expression was higher in TLS-associated hotspot spots than in non-hotspot spots (P = 5.75e-11). ZNF521, TRPA1 and GSDME also differed by hotspot status in earlier output tables, but directions and biological interpretation were less consistent. The strongest interpretable finding was therefore SDC1 enrichment within computational TLS-associated regions.

3.4 Spatial niches supported stromal and immune organization

Spatial niche analysis showed that candidate gene expression was not randomly distributed across tissue architecture. TLS-associated hotspot spots were enriched in stromal and immune-associated regions, consistent with the expected location of immune-organized microenvironmental structures. These results support a model in which SDC1 marks spatially organized tumor-microenvironment interactions in TNBC tissue.

Because the analysis used transcriptional markers rather than pathology-confirmed lymphoid aggregates, the term "TLS-associated transcriptional hotspot" was used throughout. This terminology preserves the spatial signal without overstating histologic confirmation.

3.5 SDC1-CD44 co-expression was positive, whereas SDC1-M2 macrophage support was weak

Ligand-receptor and co-expression analyses identified SDC1-CD44 as a plausible spatial association. SDC1 and CD44 showed positive spatial co-expression (Spearman r = 0.3307, P = 1.69e-130), supporting a candidate axis for further experimental investigation. However, co-expression does not establish ligand-receptor activation or causal signaling.

The SDC1-M2 macrophage relationship did not support a strong positive mechanism. SDC1 showed a weak negative correlation with the M2 macrophage score (Spearman r=-0.0336, P = 0.0165). This result argues against presenting SDC1 as a clearly positive driver of M2 macrophage enrichment in the available spatial dataset.

3.6 Drug-target and mediation findings were hypothesis-generating

The drug-target output mapped candidate genes to anesthetic and perioperative drug labels, but the repeated gene-level effect estimates across multiple drug labels indicated that these results should be treated as drug-target annotation rather than strict MR evidence. Mediation outputs were also interpreted conservatively because unstable mediation proportions can reflect weak assumptions, imprecision or incompatible total and indirect effects.

Together, these analyses are useful for prioritizing future pharmacologic and experimental studies, but they do not justify clinical treatment claims.

4. Discussion

This conservative reappraisal identifies SDC1 as the most supportable anesthesia-associated candidate gene in the available TNBC spatial transcriptomic data. The main strength of the revised evidence is not a definitive genetic causal result, but the convergence of patient-level spatial autocorrelation, TLS-associated hotspot enrichment and SDC1-CD44 spatial co-expression. These findings suggest that SDC1 may mark a spatially organized tumor-microenvironment state in TNBC.

The study also demonstrates why evidence classification is necessary in public-data multi-omics manuscripts. The available genetic outputs were insufficient for strong TNBC metastasis causality claims for SDC1, ZNF521, LPO, TRPA1 or GSDME. Overall breast cancer GWAS results cannot be assumed to represent TNBC-specific metastasis or recurrence. Similarly, drug-target annotation cannot be treated as drug-target MR without valid exposure instruments, and mediation outputs with unstable proportions should not be presented as mechanistic proof.

Spatial transcriptomics partly addresses these limitations by offering tissue-level context. SDC1 was spatially clustered in all three patients and showed enrichment in TLS-associated transcriptional hotspots. SDC1 has known relevance as a cell-surface proteoglycan and CD138 marker, and its spatial relationship with CD44 may reflect tumor-stromal or tumor-immune interface biology. However, the

current analysis cannot determine whether SDC1 is a driver, consequence or marker of these microenvironmental states.

The TLS-associated hotspot findings should also be interpreted carefully. The analysis identified a computational transcriptional pattern, not pathology-confirmed tertiary lymphoid structures. The uneven distribution of hotspot spots across patients indicates heterogeneity rather than a universal TNBC feature. This heterogeneity is biologically plausible and relevant, but it requires validation in larger spatial or histologic cohorts.

The revised manuscript therefore positions the work as an exploratory multi-omics prioritization study. This framing is more consistent with the current evidence than claims of anesthesia-induced TNBC metastasis or clinically actionable drug targeting. The results provide a rational basis for future validation of SDC1 and related spatial immune niches using TNBC-specific genetic endpoints, independent cohorts and experimental assays.

5. Limitations

Several limitations should be considered. First, the available GWAS outcome represented overall breast cancer rather than TNBC-specific metastasis or recurrence. Second, complete real-data MR support was not available for the principal spatial candidates in the analyzed resources, limiting causal interpretation. Third, the spatial transcriptomic dataset included three TNBC patients; therefore, patient-level analyses were emphasized, but larger cohorts are needed. Fourth, TLS-associated hotspots were computationally inferred and were not pathology-confirmed tertiary lymphoid structures. Fifth, independent external clinical validation and wet-lab experimental validation were not included in the retained evidence. Future work should incorporate TNBC-specific genetic outcomes, independent expression and survival cohorts, and IHC, IF, qPCR, Western blot or functional assays.

6. Conclusions

Using a conservative evidence framework, this study prioritizes SDC1 as the strongest currently supportable anesthesia-associated candidate gene in TNBC spatial transcriptomic data. The evidence supports spatial organization and TLS-associated enrichment rather than definitive causality. These results provide a focused basis for future TNBC-specific genetic validation and experimental investigation of SDC1-centered tumor-microenvironment biology.

Declarations

Ethics approval and consent to participate:

Not applicable. This study used publicly available de-identified datasets (GWAS Catalog GCST010098; GEO GSE210616).

Consent for publication:

Not applicable.

Competing interests:

The authors declare no competing interests.

Funding:

This research received no specific grant from any funding agency in the public, commercial or not-for-profit sectors.

Author Contribution

Weixian Xie: Conceptualization, Methodology, Software, Formal analysis, Data curation, Writing – original draft, Writing – review & editing, Supervision, Project administration. Wenyue Xiang: Resources, Supervision, Writing – review & editing. Zhiming Huang: Data curation, Validation, Visualization, Writing – review & editing. All authors reviewed and approved the final manuscript.

Acknowledgments:

The authors thank the contributors of the public GWAS, eQTL and spatial transcriptomic datasets used in this study.

Availability of data and materials:

Public data used in this study include GWAS Catalog accession GCST010098 and GEO accession GSE210616. Processed supplementary tables, figure files and reproducibility scripts are provided with the submission package.

References

1. Bassiouni R, Idowu MO, Bao R et al. Spatially resolved transcriptomics reveals prognostic significance of tumor microenvironment in breast cancer. Cancer Res. 2023;83(7 Suppl):Abstract nr 2282.
2. Benjamini Y, Hochberg Y. Controlling the false discovery rate: a practical and powerful approach to multiple testing. J R Stat Soc Ser B Methodol. 1995;57:289–300.

3. Bianchini G, Balko JM, Mayer IA, Sanders ME, Gianni L. Triple-negative breast cancer: challenges and opportunities of a heterogeneous disease. Nat Rev Clin Oncol. 2016;13:674–90.
4. Bowden J, Davey Smith G, Haycock PC, Burgess S. Consistent estimation in Mendelian randomization with some invalid instruments using a weighted median estimator. Genet Epidemiol. 2016;40:304–14.
5. Burgess S, Bowden J, Fall T, et al. Sensitivity analyses for robust causal inference from Mendelian randomization analyses with multiple genetic variants. Stat Med. 2017;36:1783–802.
6. Cabrita R, Lauss M, Sanna A, et al. Tertiary lymphoid structures improve immunotherapy and survival in melanoma. Nature. 2020;577:561–5.
7. Dent R, Trudeau M, Pritchard KI, et al. Triple-negative breast cancer: clinical features and patterns of recurrence. Clin Cancer Res. 2007;13:4429–34.
8. Foulkes WD, Smith IE, Reis-Filho JS. Triple-negative breast cancer. N Engl J Med. 2010;363:1938–48.
9. GTEx Consortium. The GTEx Consortium atlas of genetic regulatory effects across human tissues. Science. 2020;369:1318–30.
10. Helmink BA, Reddy SM, Gao J, et al. B cells and tertiary lymphoid structures potentiate response to checkpoint blockade in immunotherapy. Nature. 2020;577:549–55.
11. Palla G, Spitzer H, Klein M, et al. Squidpy: a scalable framework for spatial omics analysis. Nat Methods. 2022;19:171–8.
12. Sessler DI, Pei L, Huang Y, et al. Recurrence of breast cancer after regional or general anaesthesia: a randomised controlled trial. Lancet. 2019;394:1807–15.
13. Stahl PL, Salmen F, Vickovic S, et al. Visualization and analysis of gene expression in tissue sections by spatial transcriptomics. Science. 2016;353:78–82.
14. Vosa U, Claringbould A, Westra HJ, et al. Large-scale cis- and trans-eQTL analyses identify variants affecting gene expression in human blood. Nat Genet. 2021;53:1300–10.
15. Wakefield J. Bayes factors for genome-wide association studies: comparison with P-values. Genet Epidemiol. 2009;33:79–86.
16. Zhang H, Ahearn TU, Lecarpentier J, et al. Genome-wide association study identifies 32 novel breast cancer susceptibility loci from both cross-population and multi-ethnic analyses. Nat Genet. 2020;52:814–24.
17. Zhu Z, Zhang F, Hu H, et al. Integration of summary data from GWAS and eQTL studies predicts complex trait gene targets. Nat Genet. 2016;48:481–7.

Tables

Table 1

Evidence classification after conservative audit

Gene	Current genetic evidence status	Patient-level spatial evidence	TLS-associated hotspot evidence	Manuscript interpretation
SDC1	Complete eQTL-supported MR result not available in analyzed resources	Mean Moran's I 0.3042; positive in 3/3 patients; FDR < 0.05 in 3/3	Higher in hotspot spots; P = 5.75e-11	Strongest spatial candidate; hypothesis-generating
ZNF521	Complete eQTL-supported MR result not available in analyzed resources	Mean Moran's I 0.0162; positive in 2/3 patients	Lower in hotspot spots; P = 2.27e-06	Exploratory candidate
LPO	Complete eQTL-supported MR result not available in analyzed resources	Mean Moran's I 0.0283; positive in 1/3 patients	No significant hotspot enrichment; P = 0.173	Exploratory candidate
TRPA1	Complete eQTL-supported MR result not available in analyzed resources	Mean Moran's I 0.0039; positive in 1/3 patients	Lower in hotspot spots; P = 2.18e-12	Exploratory candidate
GSDME	Complete eQTL-supported MR result not available in analyzed resources	Mean Moran's I 0.0364; positive in 2/3 patients	Lower in hotspot spots; P = 1.86e-04	Exploratory candidate
SCN9A	Complete real-data MR pipeline-level finding available	Not assessed in retained spatial summary	Not assessed	Pipeline-level genetic finding only

Table 2

Patient-level Moran's I summary for selected genes

Gene	Patients	Mean Moran's I	Range of Moran's I	Positive direction	FDR < 0.05	Interpretation
SDC1	3	0.3042	0.2261 to 0.3948	3/3	3/3	Consistent positive spatial clustering
ZNF521	3	0.0162	-0.0004 to 0.0390	2/3	1/3	Mixed or patient-dependent spatial signal
LPO	3	0.0283	-0.0070 to 0.0926	1/3	1/3	Mixed or patient-dependent spatial signal
TRPA1	3	0.0039	-0.0008 to 0.0086	1/3	1/3	Mixed or patient-dependent spatial signal
GSDME	3	0.0364	-0.0005 to 0.0734	2/3	2/3	Mixed or patient-dependent spatial signal
ALDH2	3	0.1154	0.0499 to 0.2180	3/3	3/3	Consistent positive spatial clustering
HIF1A	3	0.1255	0.0838 to 0.1909	3/3	3/3	Consistent positive spatial clustering

Table 3

Spatial correlation checks

Analysis	Effect estimate	P value	Interpretation
SDC1-CD44 spatial co-expression	Spearman r = 0.3307	1.69e-130	Positive spatial association; not proof of ligand-receptor activation
SDC1-M2 macrophage score	Spearman r=-0.0336	0.0165	Weak negative association; does not support a strong positive M2 mechanism
SDC1 in TLS-associated hotspots	Higher in hotspots	5.75e-11	Supports SDC1 enrichment in computational TLS-associated regions

Figures

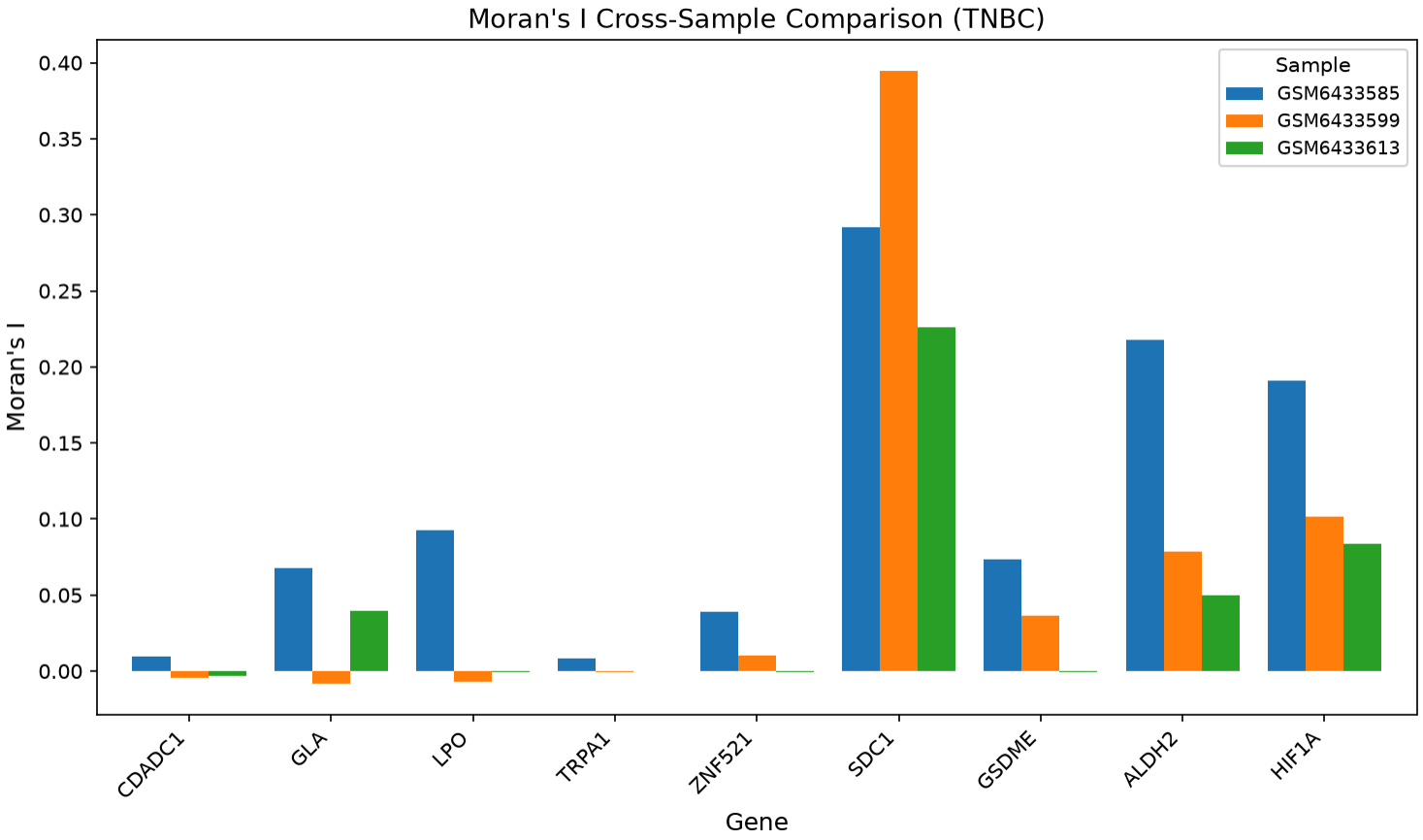


Figure 1

Patient-level Moran's I summary for anesthesia-associated candidate genes in TNBC spatial transcriptomic samples. SDC1 shows the most consistent positive spatial autocorrelation across the three patients.

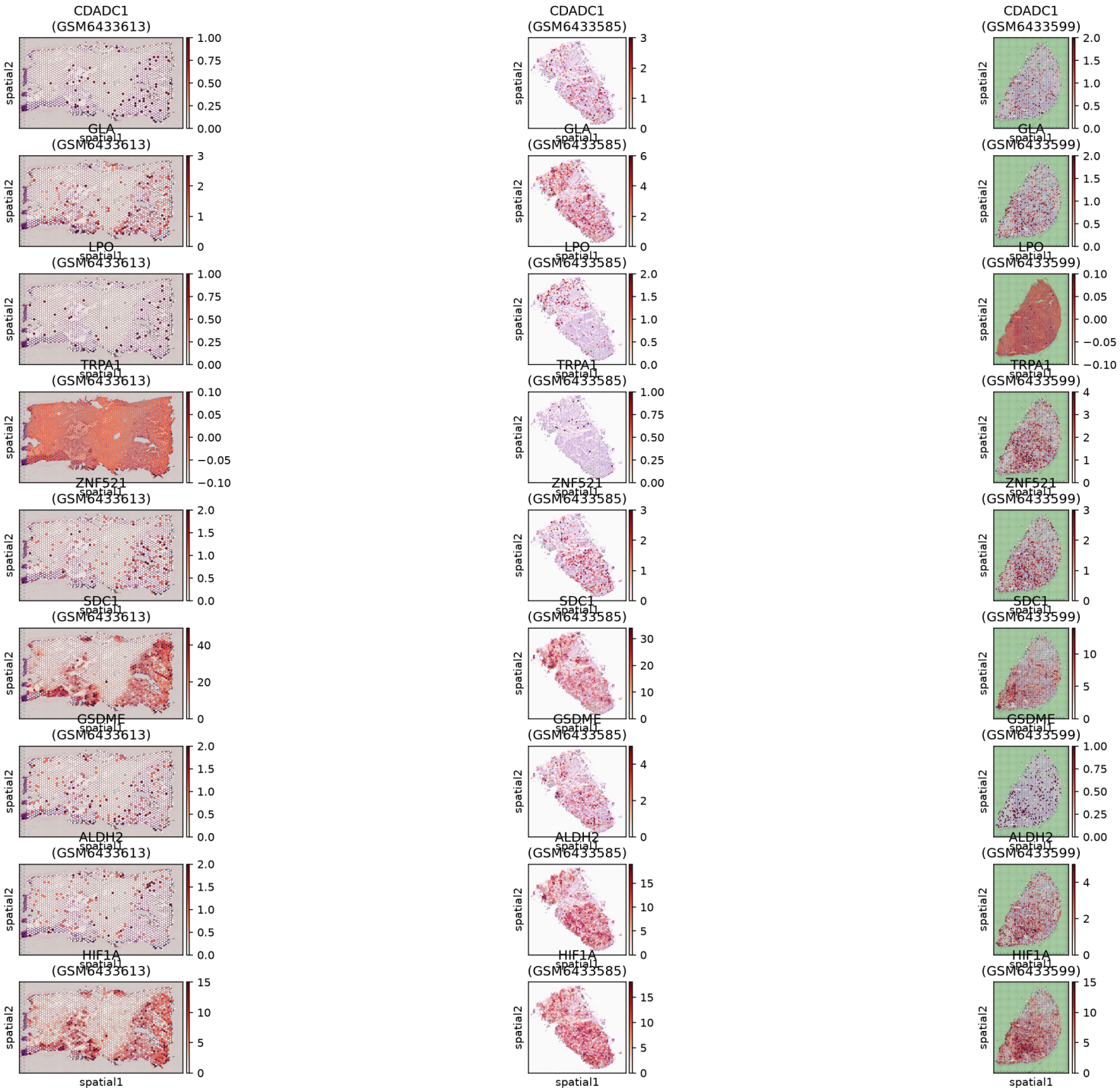


Figure 2

Spatial expression of candidate genes in TNBC tissue sections. The figure shows patient-level spatial distribution of selected anesthesia-associated candidate genes.

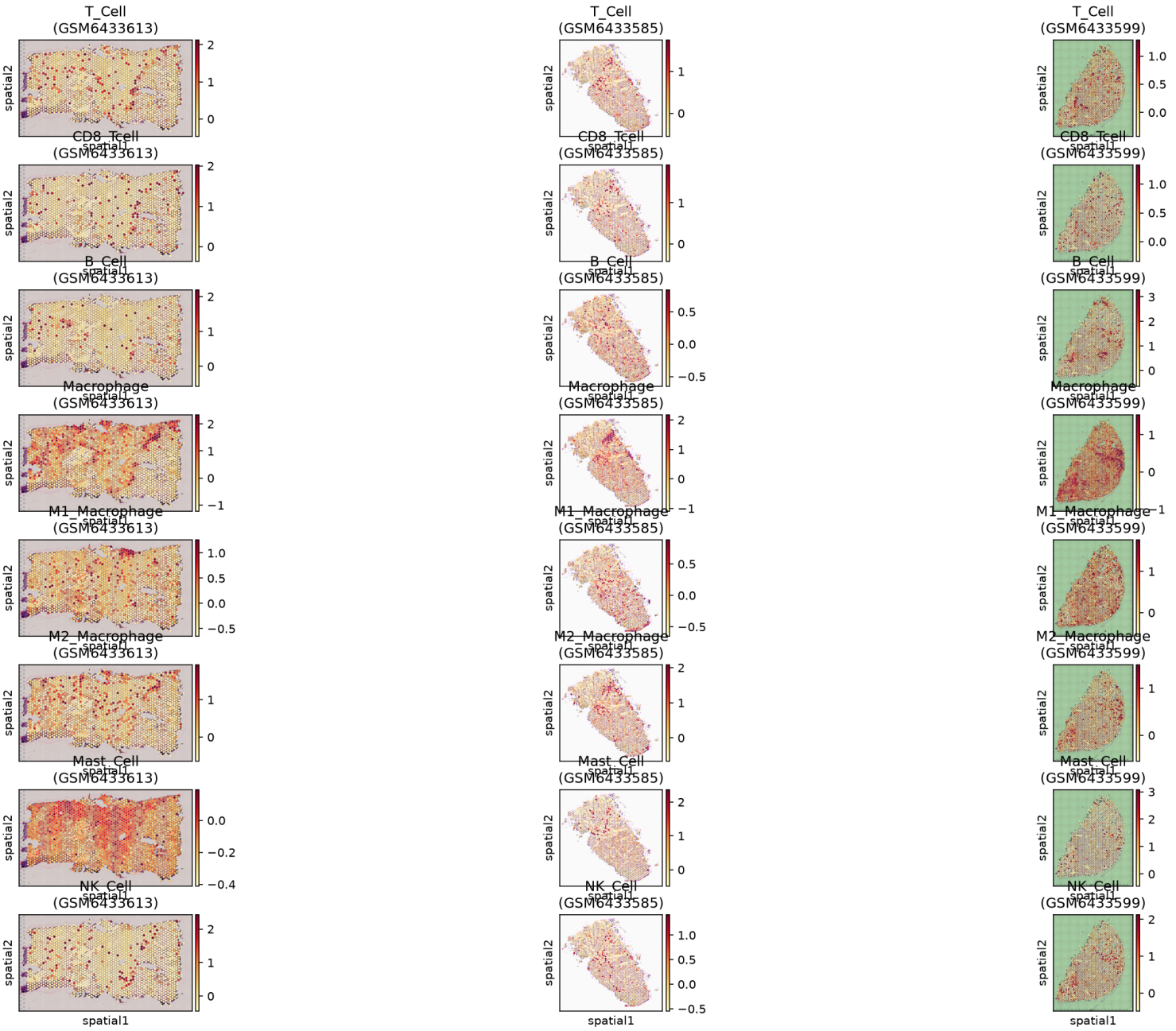


Figure 3

Immune and stromal spatial patterns in TNBC tissue. Spatial immune signatures were interpreted as marker-based transcriptional scores rather than pathology-confirmed cell states.

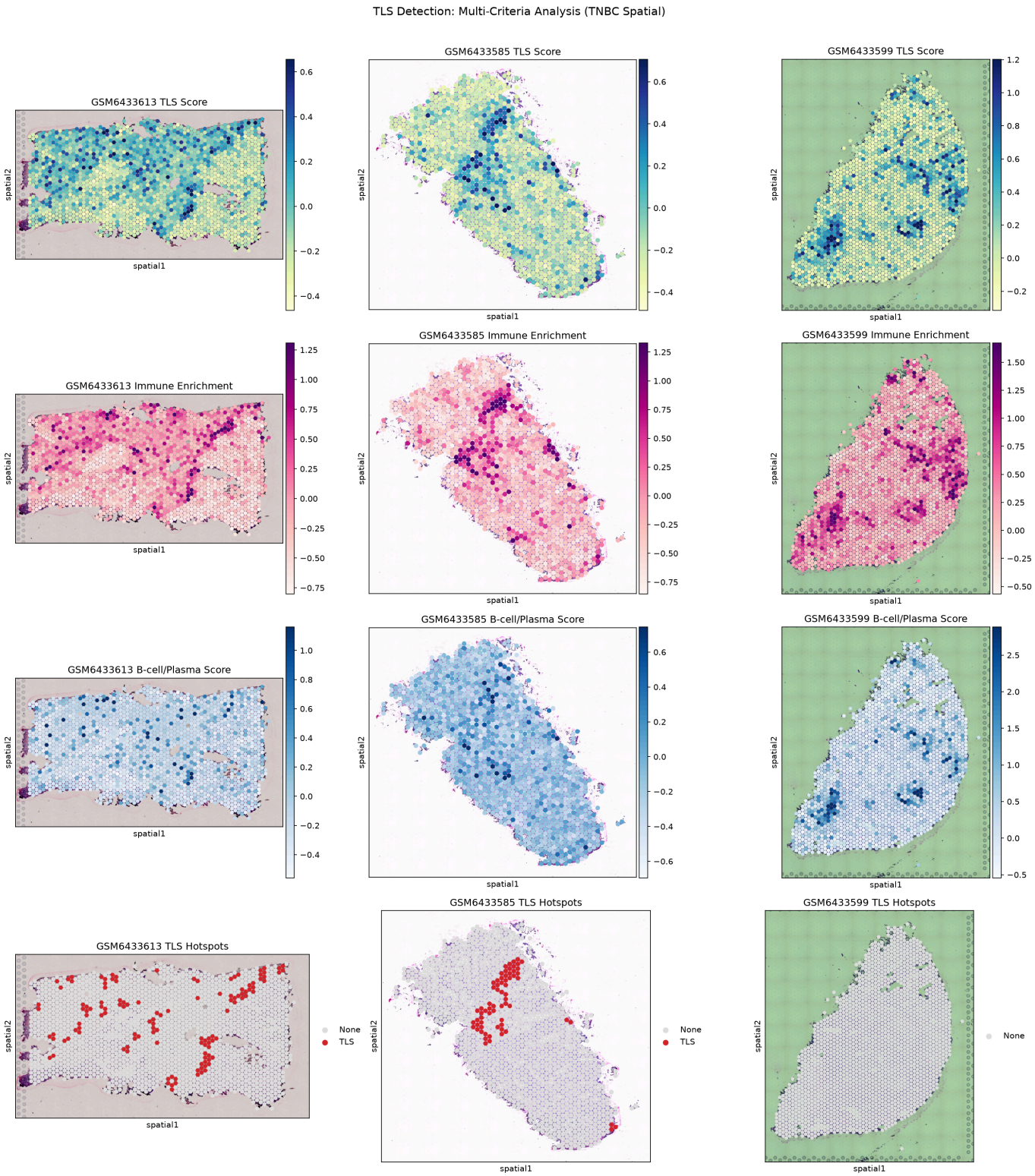


Figure 4

TLS-associated transcriptional hotspot analysis. Hotspots were computationally defined and were unevenly distributed across patients, supporting patient heterogeneity.

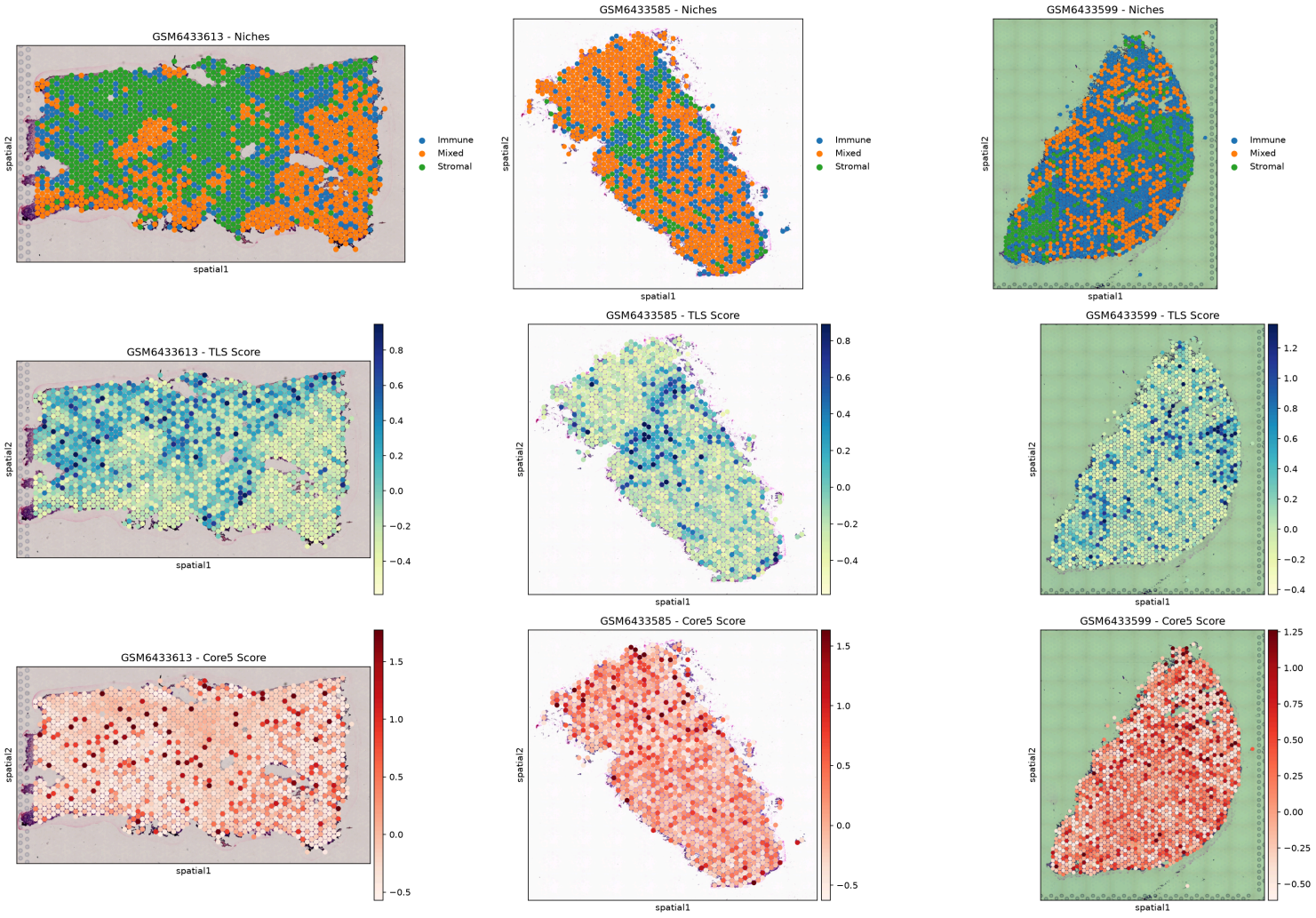


Figure 5

Spatial niche communication and candidate ligand-receptor co-expression patterns. SDC1-CD44 co-expression was interpreted as spatial association and not as causal ligand-receptor activation.

Supplementary Files

This is a list of supplementary files associated with this preprint. Click to download.

- SupplementaryTables.xlsx
- FigureS1TLSHotspotsOptimized.png